

## Supplemental Materials and Methods

The MS1 mouse endothelial cell line was obtained from the American Type Culture Collection (ATCC, Manassas, VA) and was grown by serial passage. Cell culture materials were purchased from Invitrogen (Life Technologies, Grand Island, NY). Chemicals, unless otherwise stated, and IgG<sub>1</sub> (Kappa from human myeloma plasma) were purchased from Sigma-Aldrich (St. Louis, MO).

## Radioimmunoassay Analysis.

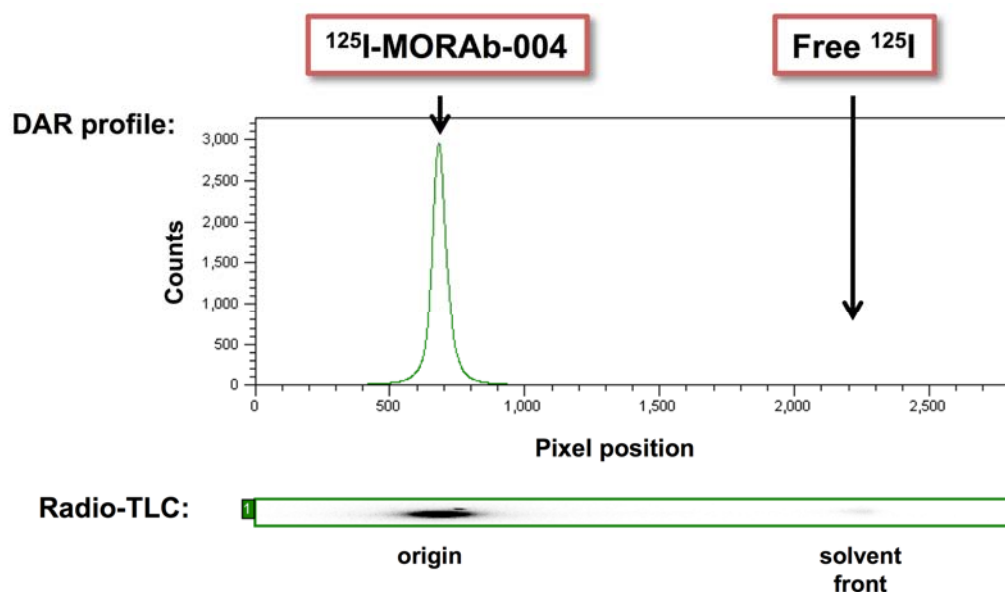
The apparent binding affinity,  $K_d$ , and the number of functional binding sites,  $B_{max}$ , for specific binding were calculated using non-linear regression analysis of a one-site binding hyperbola equation and Scatchard analysis, as previously described.  $K_d$  and  $B_{max}$  values are presented as the mean  $\pm$  S.D. of three or more independent experiments, and each independent experiment was performed in quadruplicate. In competitive binding assays, the observed specific binding was plotted as a function of unlabeled mAb concentration. The  $K_i$  for unlabeled MORAb-004 was determined by fitting this data to a “four-parameter logistic non-linear regression model” most commonly used for sigmoidal curves, where  $K_d$  is the dissociation binding constant of  $^{125/124}\text{I}$ -MORAb-004 determined from the direct binding study and  $K_i = \text{IC}_{50}/(1 + [\text{mAb}]/K_d)$ .

## Blood Pharmacokinetics

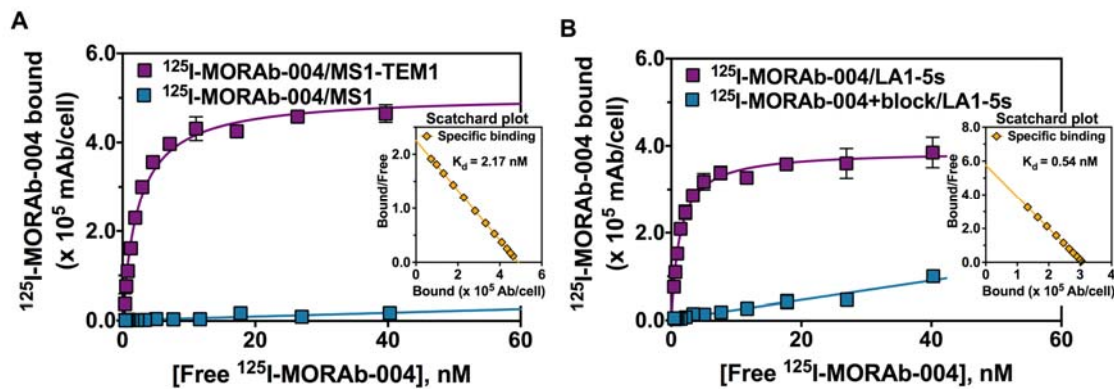
Naïve *nu/nu* female mice and *nu/nu* female mice bearing ID8 tumors co-mixed with MS1 or MS1-TEM1 cells were administered  $^{125}\text{I}$ -MORAb-004 (0.185 MBq [5  $\mu\text{Ci}$ ], 2.5  $\mu\text{g}$  of mAb, in 150  $\mu\text{L}$  of sterile 0.9% saline for injection) via the tail vein (0 h). Blood samples were collected at designated time points by retro-orbital puncture (2, 5, 10, 15, 30, 60, 240, 360, 1440, 2880, and 4320 min), weighed, and radioactivity levels measured by a  $\gamma$ -counter. Blood activity levels were normalized to mouse weight to determine the percent injected dose per organ (% ID/org). Data was fit to bi-exponential decay curves using Prism 5.0 (GraphPad) software, where the  $\alpha$ - and  $\beta$ -decay rates for blood clearance were extrapolated.

## Immunohistochemistry

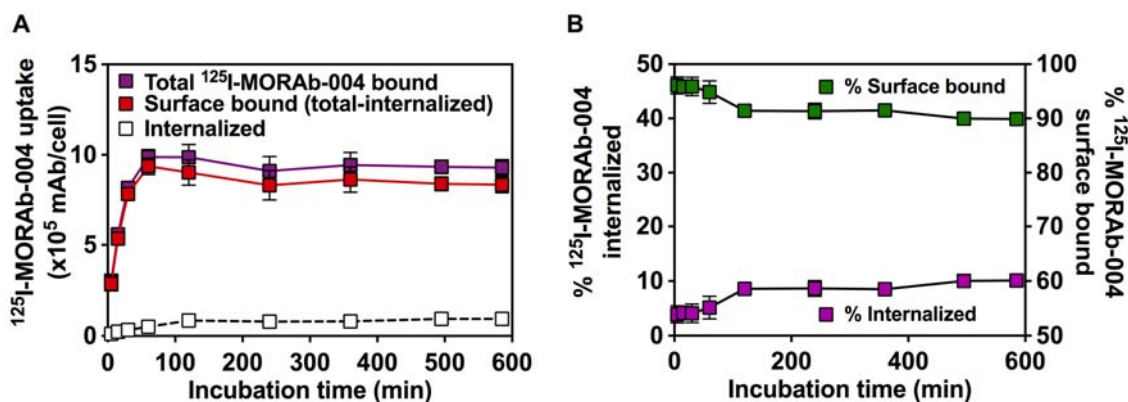
Tumor sections were cut at 5  $\mu$ m thickness onto glass slides and were single immunostained by incubating with rabbit anti-TEM1 polyclonal antibody (Morphotek) followed by goat anti-rabbit HRP-conjugated antibody, with DAB Chromagen (Dako) used as the detection reagent. Slides were scanned on a whole-slide imaging system (Aperio).



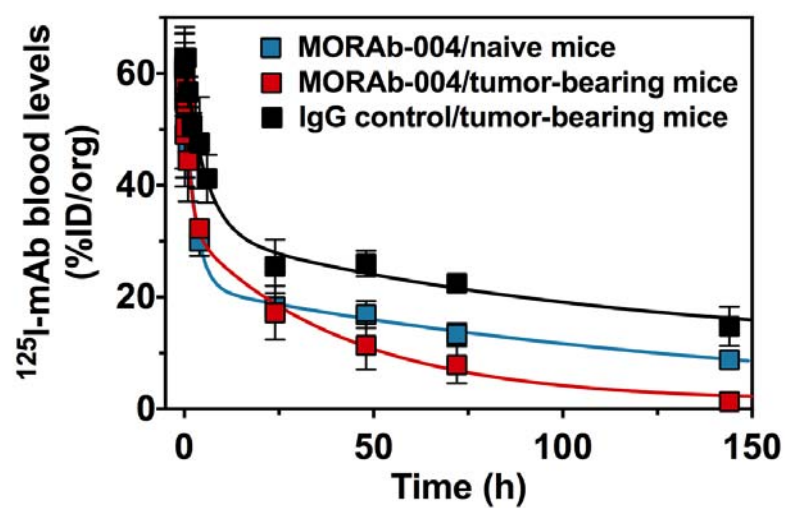
**Supplemental Figure 1.** Representative radioTLC and DAR chromatogram of purified <sup>125</sup>I-MORAb-004 post purification by spin desalting column. Employing 4:1 MeOH in water as the eluant, the labeled antibody remains at the baseline ( $R_f = 0.0$ ) origin, whereas free radioiodide travels to solvent front ( $R_f = 1.0$ ).



**Supplemental Figure 2.** Cell surface binding of  $^{125}\text{I}$ -MORAb-004 to (A) recombinant hTEM1 on live MS1-TEM1/MS1 murine endothelial cells and (B) native hTEM1 on live LA1-5s human neuroblastoma cancer cells was determined by RIA. Cells were incubated with increasing concentrations of mAb and incubated for 4 h at 4°C. The apparent  $K_d$  of  $^{125}\text{I}$ -MORAb-004 for endogenous hTEM1 is lower than that for recombinant hTEM1 (0.54 nM versus 2.17 nM respectively).



**Supplemental Figure 3.** Internalization of  $^{125}\text{I}$ -MORAb-004 in LA1-5s cells with respect to the total amount of mAb bound per cell following incubation at 37°C as a function of time. (A) Internalization was measured in presence or absence of an excess of unlabeled MORAb-004 (100 nM) in incubation medium to block hTEM1 surface protein binding. (B) Internalized fraction of  $^{125}\text{I}$ -MORAb-004 over time as a function of total cell-associated radioactivity. Values shown are mean of three independent experiments performed in quadruplicate.

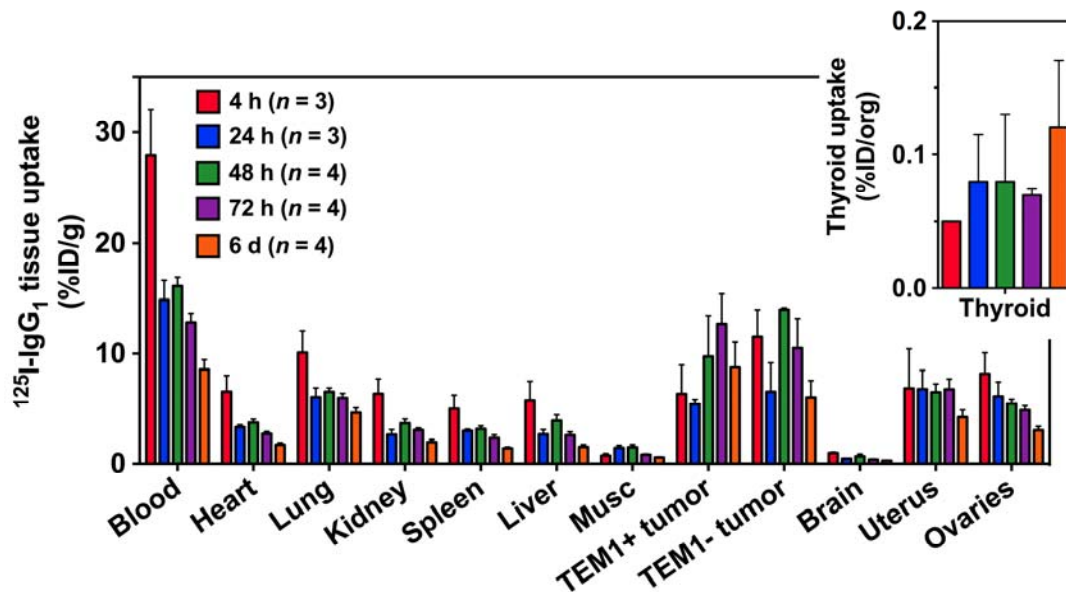


**Supplemental Figure 4.** *In vivo* blood pharmacokinetics of  $^{125}\text{I}$ -MORAb-004 in naïve and MS1/ID8 tumor-bearing *nu/nu* female mice. %ID/Org data are fit to bi-exponential decay curve to obtain both the  $\alpha$ - and  $\beta$ -phase of blood clearance kinetics of MORAb-004.

**SUPPLEMENTAL TABLE 1**

Blood Pharmacokinetics Parameters of  $^{125}\text{I}$ -MORAb-004 and Isotype Control  $^{125}\text{I}$ -IgG  
in Naïve *versus* Tumor-Bearing *nu/nu* Female Mice

Half Life (min)	$^{125}\text{I}$ -MORAb-004		Control $^{125}\text{I}$ -IgG <sub>1</sub>
	Naïve Mice	Tumor-Bearing Mice	Tumor-Bearing Mice
$\beta$ Decay (Slow)	117.9	28.8	76.9
$\alpha$ Decay (Fast)	1.9	1.1	3.7
R <sup>2</sup>	0.95	0.92	0.96



**Supplemental Figure 5.** Biodistribution (%ID/g) of isotype control  $^{125}\text{I}$ -IgG<sub>1</sub> (2.5  $\mu\text{g}/\text{mouse}$ ) in MS1-TEM1/ID8 and MS1/ID8 tumor-bearing *nu/nu* female mice. Inset is uptake of radioiodine in thyroid (%ID/organ).



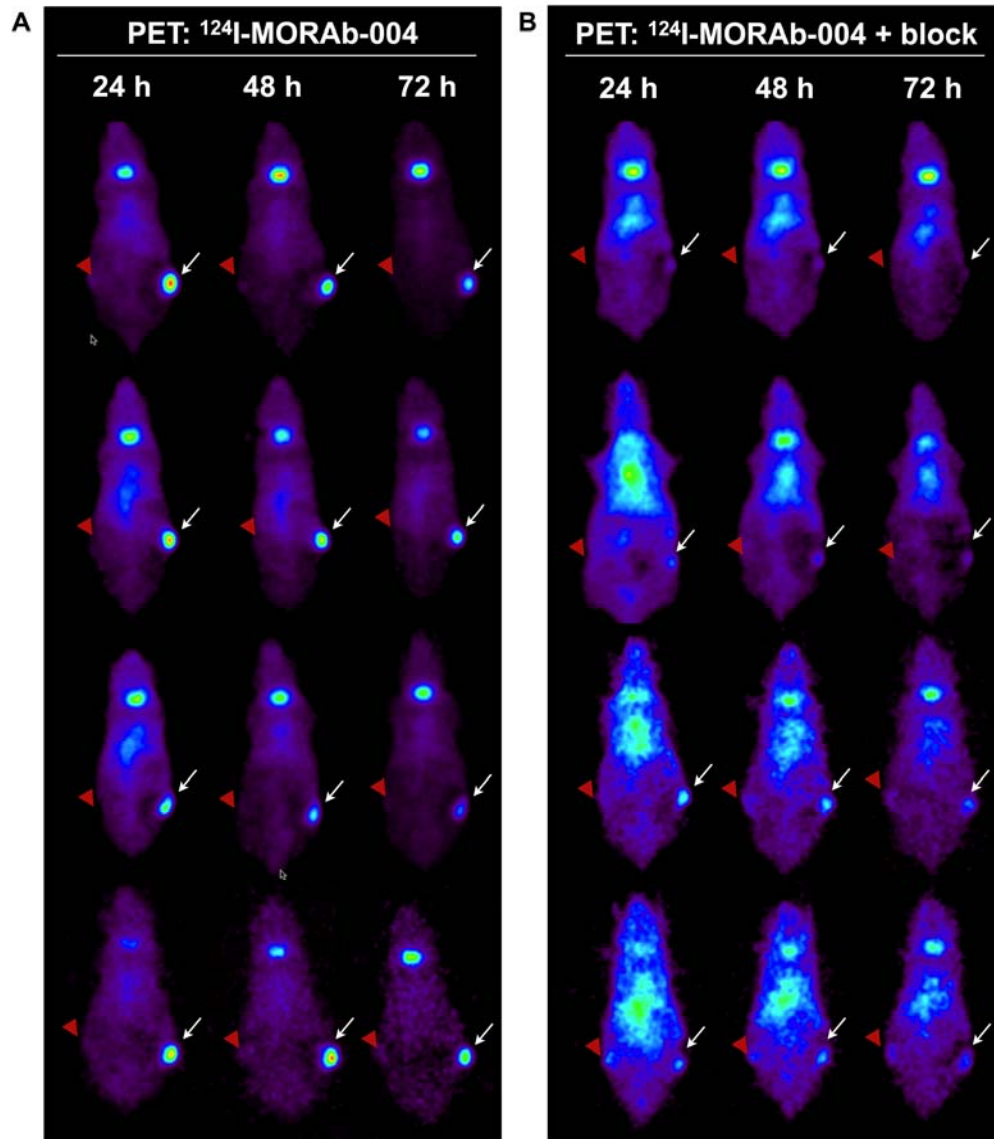
# SUPPLEMENTAL TABLE 2

Biodistribution Data of  $^{125}\text{I}$ -IgG<sub>1</sub> Administered Intravenously to Mice Bearing Subcutaneous MS1-TEM1/ID8 and MS/ID8 Tumors\*

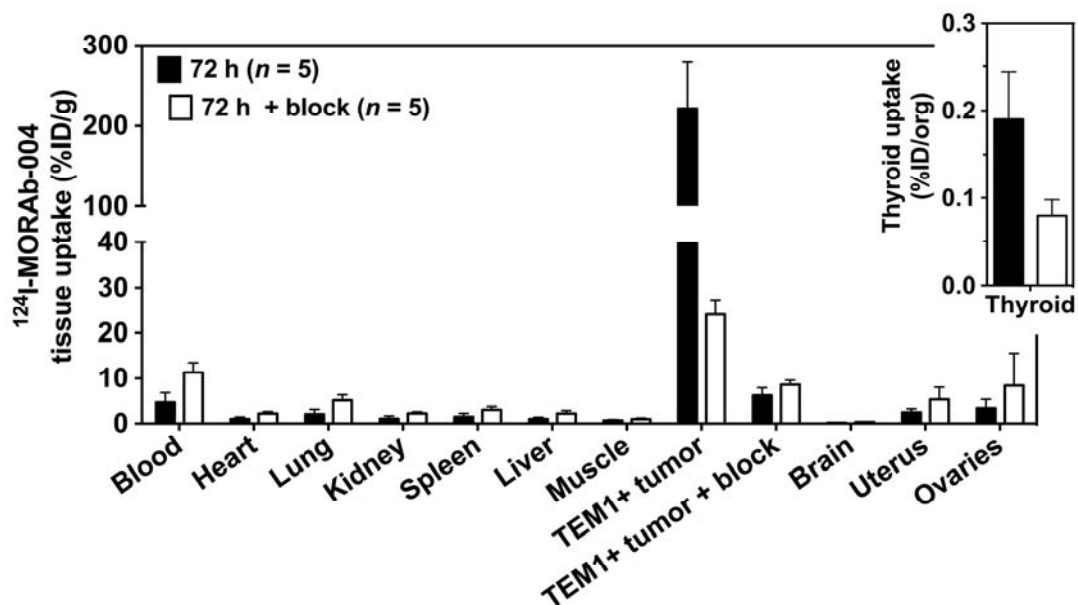
Organ	4 h (n = 3)		24 h (n = 3)		48 h (n = 4)		72 h (n = 4)		6 d (n = 4)	
Blood	27.92	± 7.19	14.83	± 3.03	16.07	± 1.55	12.78	± 1.63	8.57	± 1.78
Heart	6.56	± 2.53	3.31	± 0.37	3.74	± 0.60	2.72	± 0.39	1.73	± 0.34
Lungs	10.09	± 3.33	6.06	± 1.45	6.55	± 0.69	5.99	± 0.82	4.64	± 0.89
Kidney	6.37	± 2.34	2.65	± 0.76	3.68	± 0.75	3.05	± 0.38	1.96	± 0.47
Spleen	5.00	± 2.16	2.98	± 0.27	3.15	± 0.55	2.34	± 0.54	1.4	± 0.26
Liver	5.77	± 2.99	2.67	± 0.74	3.91	± 1.06	2.59	± 0.58	1.53	± 0.41
Muscle	0.75	± 0.31	1.45	± 0.28	1.50	± 0.48	0.83	± 0.13	0.58	± 0.11
Brain	0.98	± 0.16	0.47	± 0.02	0.67	± 0.44	0.39	± 0.10	0.28	± 0.07
Uterus	6.86	± 6.22	6.79	± 2.95	6.51	± 1.52	6.78	± 1.86	4.23	± 1.31
Ovaries	8.18	± 3.29	6.13	± 2.28	5.48	± 0.77	4.88	± 0.80	3.04	± 0.68
Thyroid <sup>†</sup>	0.05	± 0.02	0.06	± 0.06	0.08	± 0.10	0.07	± 0.01	0.12	± 0.1
Tumors										
MS1-TEM1/ID8	6.36	± 4.53	5.43	± 0.70	9.75	± 7.29	12.64	± 5.46	8.76	± 4.61
MS1/ID8	11.53	± 4.15	6.55	± 4.55	13.93	± 0.34	10.52	± 5.20	6.03	± 3.04
Ratio of TEM1+ Tumor to:										
Blood	0.23	± 0.17	0.37	± 0.09	0.61	± 0.46	0.99	± 0.45	1.02	± 0.58
Muscle	8.48	± 6.98	3.74	± 0.87	6.50	± 5.29	15.23	± 7.00	15.10	± 8.45
TEM1- Tumor	0.55	± 0.44	0.83	± 0.59	0.70	± 0.52	1.20	± 0.79	1.45	± 1.06

\*Data are expressed as %ID/g ± S.D.

<sup>†</sup>Data are expressed as %ID/Org ± S.D.



**Supplemental Figure 6.** Longitudinal *in vivo* Immuno-PET imaging of  $^{124}\text{I}$ -MORAb-004 in nude mice bearing subcutaneous chimeric ID8 tumor grafts over time. Mice ( $n=4$ ) were injected with  $^{124}\text{I}$ -MORAb-004 (5.2 MBq, 2.5  $\mu\text{g}$  mAb) (A) or co-injected with a blocking dose of 25  $\mu\text{g}$  of unlabeled MORAb-004 (B) and scanned for 1 hour at different time points post-injection. PET images from mice in each group are shown. (A) Increased uptake of  $^{124}\text{I}$ -MORAb-004 was observed in tumors expressing MS1-TEM1/ID8 tumor (right, white arrow), compared with control MS1/ID8 tumor (left, left arrowhead). (B) Specific blocking of  $^{124}\text{I}$ -MORAb-004 uptake in TEM1+ tumor observed following administration of excess MORAb-004.



**Supplemental Figure 7.** *Ex vivo* tissue activity levels of  $^{124}\text{I}$ -MORAb-004 in mice bearing subcutaneous MS1-TEM1/ID8 and MS1/ID8 tumors at 72 h  $\pm$  MORAb-004 blocking. There was a significant difference between uptake in TEM1+ tumors as compared to TEM1+ tumor+ block. P-value < 0.001.

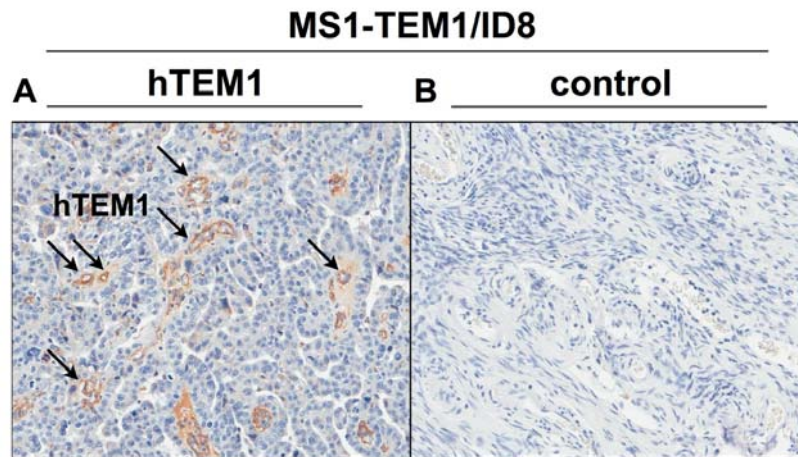
### SUPPLEMENTAL TABLE 3

Biodistribution Data of  $^{124}\text{I}$ -MORAb-004 Post PET in Mice Bearing Subcutaneous MS1-TEM1/ID8 and MS/ID8 Tumors\*

Organ	72 h ( <i>n</i> = 5)	72 h + Block ( <i>n</i> = 5)
Blood	4.65 ± 2.16	11.36 ± 2.16
Heart	1.03 ± 0.44	2.23 ± 0.46
Lungs	2.07 ± 1.10	5.11 ± 1.23
Kidney	1.09 ± 0.61	2.28 ± 0.36
Spleen	1.53 ± 0.74	3.07 ± 0.75
Liver	1.00 ± 0.42	2.25 ± 0.65
Muscle	0.72 ± 0.19	0.99 ± 0.27
Brain	0.17 ± 0.05	0.34 ± 0.08
Uterus	2.51 ± 0.79	5.31 ± 2.73
Ovaries	3.46 ± 1.87	8.39 ± 7.21
Thyroid <sup>†</sup>	0.12 ± 0.19	0.04 ± 0.08
Tumors		
MS1-TEM1/ID8	221.82 ± 57.33	24.06 ± 3.26
MS1/ID8	6.22 ± 1.69	8.60 ± 1.01
Ratio of TEM1+ Tumor to:		
Blood	47.70 ± 25.36	2.12 ± 0.49
Muscle	308.08 ± 113.80	24.30 ± 7.40
TEM1- Tumor	35.66 ± 13.37	2.80 ± 0.50

\*Data are expressed as %ID/g ± S.D.

<sup>†</sup>Data are expressed as %ID/Org ± S.D.



**Supplemental Figure 8.** (A) Human TEM1 (hTEM1)-immunostaining of mouse tumor section with rabbit anti-TEM1 polyclonal antibody. Positive staining of subcutaneous ID8 tumors enriched with MS1-TEM1/fLuc endothelial cells shows that MS1-TEM1/fluc cells form vascular capillaries (arrows). (B) Lack of nonspecific staining is observed in MS1-TEM1/ID8 tumor sections incubated with secondary goat anti-rabbit HRP-conjugated antibody alone, followed by incubation with detection reagents. Images represent approximately 25% of a 20x magnification.